Coupled Harmonic Bases for Longitudinal Characterization of Brain Networks (Supplemental Material)

Seong Jae Hwang[1] Nagesh Adluru[4] Maxwell D. Collins[1] Sathya N. Ravi[1]
Barbara B. Bendlin[3] Sterling C. Johnson[3] Vikas Singh[2,1]

[1]Dept. of Computer Sciences, University of Wisconsin – Madison
[2]Dept. of Biostatistics and Med. Informatics, University of Wisconsin – Madison
[3]William S. Middleton VA Hospital, Madison, WI [4]Waisman Center, University of Wisconsin – Madison

In this supplemental material, we first provide an additional procedure in our algorithm that effectively deals with the singular matrices. Next, we briefly show the scaling aspect of our algorithm. Then, we show the accuracy results for two additional cognitive tests. Lastly, we demonstrate how we rotate the "knob" to see the global change of the brain connectivity with an interactive visualization provided as an html script (`index.html`).

1. Singularity Correction

In the paper, we have been assuming that H in (16) derived from the newly represented constraint is nonsingular, allowing us to perform inversions in the subsequent steps. However, even if the initial H is nonsingular, we cannot guarantee to maintain its nonsingularity throughout the iterations. Thus, we now relax that assumption in the previous procedures to consider singular H in the subproblems.

First, we factor out the submatrix of our interest, $M_{\mathcal{SS}}$ of size $s \times p$, from (16) and rewrite it as

$$\left(V_{\mathcal{S}\cdot} + M_{\mathcal{SS}}^{-1} M_{\bar{\mathcal{S}}\mathcal{S}}^T V_{\bar{\mathcal{S}}\cdot}\right)^T M_{\mathcal{SS}} \left(V_{\mathcal{S}\cdot} + M_{\mathcal{SS}}^{-1} M_{\bar{\mathcal{S}}\mathcal{S}}^T V_{\bar{\mathcal{S}}\cdot}\right) = H. \tag{1}$$

Then, iff $V_{\mathcal{S}\cdot} + M_{\mathcal{SS}}^{-1} M_{\bar{\mathcal{S}}\mathcal{S}}^T V_{\bar{\mathcal{S}}\cdot}$ is nonsingular, H will be nonsingular for any submatrix $M_{\mathcal{SS}}$. Thus, to apply the *singularity correction*, we rearrange the columns of $M_{\mathcal{SS}}$ to get a new submatrix containing the maximal set of linearly independent columns of the subproblem adjacently. First, assume w.l.o.g. that

$$V_{\mathcal{S}\cdot} + M_{\mathcal{SS}}^{-1} M_{\bar{\mathcal{S}}\mathcal{S}}^T V_{\bar{\mathcal{S}}\cdot} = \begin{bmatrix} U & UC \end{bmatrix} \tag{2}$$

for a $s \times r$ nonsingular matrix U and a $r \times (p-r)$ matrix C. Then, for $\mathcal{T}$, the indices of the columns of U, we have

$$U = V_{\mathcal{S}\mathcal{T}} + M_{\mathcal{SS}}^{-1} M_{\bar{\mathcal{S}}\mathcal{S}}^T V_{\bar{\mathcal{S}}\mathcal{T}} \tag{3}$$

which allows us to write (1) as follows:

$$\begin{bmatrix} U & UC \end{bmatrix}^T M_{\mathcal{SS}} \begin{bmatrix} U & UC \end{bmatrix} = \begin{bmatrix} U^T M_{\mathcal{SS}} U & U^T M_{\mathcal{SS}} UC \\ C^T U^T M_{\mathcal{SS}} U & C^T U^T M_{\mathcal{SS}} UC \end{bmatrix} = H. \tag{4}$$

Treating C as a fixed constant, the equality (1) can be reduced to consider only the linearly independent columns $\mathcal{T}$ of the submatrix U as

$$\left(V_{\mathcal{S}\mathcal{T}} + M_{\mathcal{SS}}^{-1} M_{\bar{\mathcal{S}}\mathcal{S}}^T V_{\bar{\mathcal{S}}\mathcal{T}}\right)^T M_{\mathcal{SS}} \left(V_{\mathcal{S}\mathcal{T}} + M_{\mathcal{SS}}^{-1} M_{\bar{\mathcal{S}}\mathcal{S}}^T V_{\bar{\mathcal{S}}\mathcal{T}}\right) = H_{\mathcal{TT}} \tag{5}$$

and (4) is true iff the above equation is true. Thus, given $U \in \mathbb{R}^{s \times r}$ such that $U^T M_{\mathcal{SS}} U = H_{\mathcal{TT}}$, the new feasible iterates for linearly independent columns $\mathcal{T}$ and their complement columns $\bar{\mathcal{T}}$ respectively are

$$V_{\mathcal{S}\mathcal{T}} = U - M_{\mathcal{SS}}^{-1} M_{\bar{\mathcal{S}}\mathcal{S}}^T V_{\bar{\mathcal{S}}\mathcal{T}}, \tag{6}$$

$$V_{\mathcal{S}\bar{\mathcal{T}}} = UC - M_{\mathcal{SS}}^{-1} M_{\bar{\mathcal{S}}\mathcal{S}}^T V_{\bar{\mathcal{S}}\bar{\mathcal{T}}}. \tag{7}$$

We note that the singularity correction is able to preserve the feasibility of the new iterate by first observing that.

$$V_{\mathcal{ST}} + M_{\mathcal{SS}}^{-1} M_{\mathcal{S}\bar{\mathcal{S}}}^T V_{\bar{\mathcal{S}}\cdot} = \left[U - M_{\mathcal{SS}}^{-1} M_{\mathcal{S}\bar{\mathcal{S}}}^T V_{\bar{\mathcal{S}}\mathcal{T}} \quad UC - M_{\mathcal{SS}}^{-1} M_{\mathcal{S}\bar{\mathcal{S}}}^T V_{\bar{\mathcal{S}}\bar{\mathcal{T}}}\right] + \left[M_{\mathcal{SS}}^{-1} M_{\mathcal{S}\bar{\mathcal{S}}}^T V_{\bar{\mathcal{S}}\mathcal{T}} \quad M_{\mathcal{SS}}^{-1} M_{\mathcal{S}\bar{\mathcal{S}}}^T V_{\bar{\mathcal{S}}\bar{\mathcal{T}}}\right] \tag{8}$$

$$= \left[U \quad UC\right]. \tag{9}$$

Thus, for any $M_{\mathcal{SS}}$, we show it is exactly the same as (4), reaffirming the next iterate feasibility. Note that we still require that $M_{\mathcal{SS}}$ to be positive definite for any $\mathcal{S}$, but this can be guaranteed by showing that

$$\mathbf{x}^T M_{\mathcal{SS}} \mathbf{x} \overset{\text{w.l.o.g.}}{=} \begin{bmatrix}\mathbf{x}\\ 0\end{bmatrix}^T \begin{bmatrix} M_{\mathcal{SS}} & M_{\bar{\mathcal{S}}\mathcal{S}}^T \\ M_{\bar{\mathcal{S}}\mathcal{S}} & M_{\bar{\mathcal{S}}\bar{\mathcal{S}}}\end{bmatrix} \begin{bmatrix}\mathbf{x}\\ 0\end{bmatrix} \geq 0.$$

2. Scaling of Stochastic Block Coordinate Descent

Below, Table 1 shows the average runtimes of the Stochastic Block Coordinate Descent (SBCD) without a regularizer for various $n \times n$ random matrices which essentially solves for the solutions of the generalized eigenvalue problems. This also gives a rough estimate of the runtime of the entire framework which involves computing multiple SBCD operations for all the partitions.

n	100	500	1000	3000	5000	7000	10000	12000
runtime (sec)	0.32	0.44	2.31	34.95	125.78	428.71	979.92	1372.83

Table 1: The average runtime of 10 SBCD operations (without a regularizer) for solving $V \in \mathbb{R}^{n\times p}$ given a $n \times n$ matrix X for $p = 20$. The iteration terminated when the objective value is with $< 5\%$ of the true objective value of GEVP.

3. Additional Cognitive Tests: Quantile Prediction Results

We also perform the quantile prediction experiments using two additional cognitive scores: Trail Making Test and Wechsler Memory Scaling - Revised Logical Memory II Test (WMSR). Both tests are designed to measure different cognitive functionalities and are often used for detecting neurological disorders such as Alzheimer's disease [1, 2]. As in the cognitive tests in the main paper (RAVLT and MMSE), the scores are normalized to account for the other nuisance covariates (age and gender) that could potentially contribute to the cognitive test scores. We have used the exact same setup as in the main paper for these tests show in Table 2 and Table 3 respectively. We observe that the overall accuracies of the both setups are lower than the cognitive tests (RAVLT and MMSE) in the main paper. Nonetheless, the coupled bases could achieve higher quantile prediction accuracies in many setups compared to the non-coupled cases.

K	Non-coupled		Coupled	
	$j = 1$	$\{1, 2, 3\}$	$j = 1$	$\{1, 2, 3\}$
2	61.90	41.27	71.43	66.67
3	42.86	33.33	42.86	41.27
4	28.57	28.57	47.62	34.92

Table 2: Prediction accuracy (%) of Trail Making Test quantiles on $j = 1$ time point and $j = \{1, 2, 3\}$ time points. K is the number of quantiles.

K	Non-couple		Coupled	
	$j = 1$	$\{1, 2, 3\}$	$j = 1$	$\{1, 2, 3\}$
2	47.62	39.68	66.67	61.90
3	47.62	28.57	47.62	41.27
4	33.33	20.63	42.86	38.10

Table 3: Prediction accuracy (%) of WMSR Test quantiles on $j = 1$ time point and $j = \{1, 2, 3\}$ time points for K quantile setups.

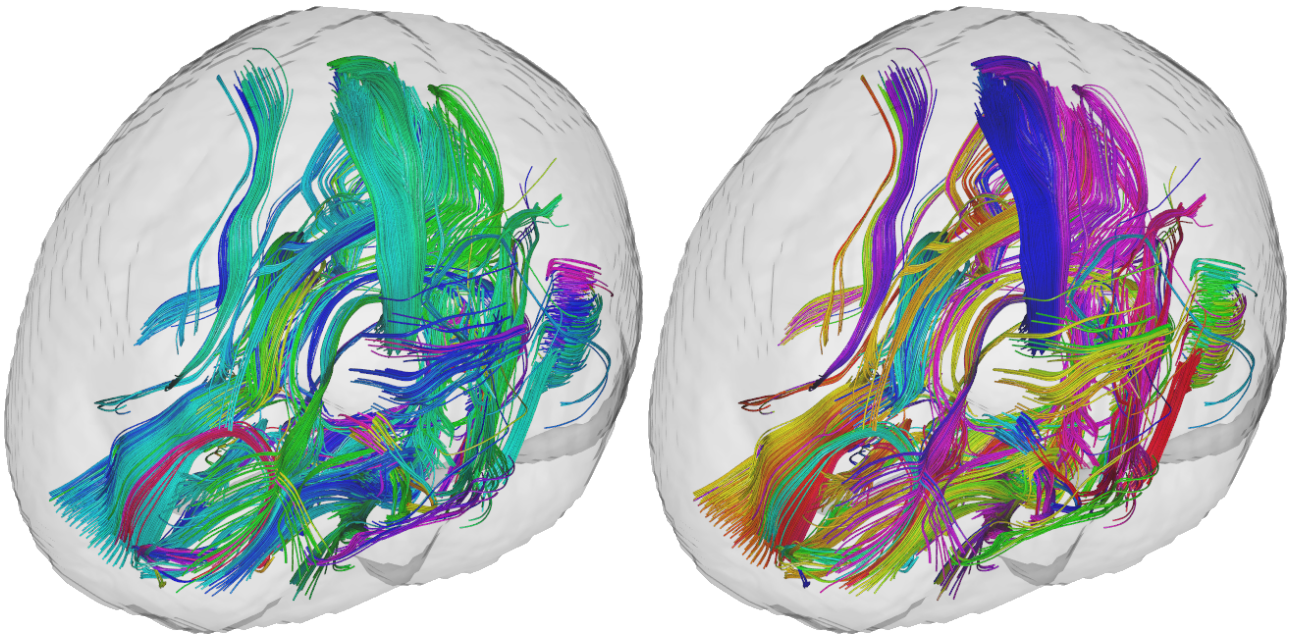

Figure 1: Left: the initial evolution stage of the top connectivities. Right: the final evolution stage of the top connectivities.

4. Interactive Brain Connectivity Evolution Visualization

In this section, we demonstrate the visualization of the brain connectivity evolution that we have found using our RAVLT cognitive score based coupling. First, we partitioned the subjects into 20 quantiles based on their RAVLT scores. Then, we have computed the coupled bases across the partitions and based on those bases, we selected the 50 edges that change the most across the partitions. The left and right images of Fig. 1 show the reconstructed fiber tracts of those top 50 edges of the brain connectivities, allowing us to visualize the anatomical structures of the connectivities.

We have provided an interactive html script (`index.html`) to demonstrate the ability to visualize the global change of the tract colors by turning a knob. In the script, we start with the left image of Fig. 1 where the evolution begins (left end of the slider) and gradually evolve towards the right image of Fig. 1 where the change ends. Note that this is just a simulation to show the possible visualization of the significant tracts that we have extracted. In the future, once we are able to control the colors of the individual tracts to reflect their connectivity strengths, we will be able to meaningfully show the local-level evolution across the quantiles and intuitively understand both local and global evolution of the brain connectivities given any covariate we desired to see the effects of.

References

[1] J. A. Arnett and S. S. Labovitz. Effect of physical layout in performance of the Trail Making Test. *Psychological Assessment*, 7(2):220, 1995. 2

[2] J. Hunsley and C. M. Lee. *Introduction to clinical psychology: An evidence-based approach*. Wiley Global Education, 2009. 2